



Riverine nutrient impact on global ocean nitrogen cycle feedbacks and marine primary production in an Earth System Model

Miriam Tivig^{1,2}, David P. Keller¹, and Andreas Oschlies¹

¹GEOMAR Helmholtz-Zentrum für Ozeanforschung Kiel, Wischhofstr. 1-3, D-24148 Kiel, Germany

²Deutscher Wetterdienst, Abteilung Klima und Umwelt, Michendorfer Chaussee 23, D-14473 Potsdam, Germany.

Correspondence: Miriam Tivig (mtivig@geomar.de)

Abstract.

Riverine nutrient export is an important process in marine coastal biogeochemistry and also impacts global marine biology. The nitrogen cycle is a key player here. Internal feedbacks regulate not only nitrogen distribution, but also primary production and thereby oxygen concentrations. Phosphorus is another essential nutrient and interacts with the nitrogen cycle via different feedback mechanisms. After a previous study of the marine nitrogen cycle response to riverine nitrogen supply, we here additionally include phosphorus from river export with different phosphorus burial scenarios and study the impact of phosphorus alone and in combination with nitrogen in a global 3-D ocean biogeochemistry model. Again, we analyse the effects on near coastal and open ocean biogeochemistry. We find that the addition of bio-available riverine phosphorus alone or together with nitrogen affects marine biology on millennial timescales more than riverine nitrogen alone. Biogeochemical feedbacks in the marine nitrogen cycle are strongly influenced by the additional phosphorus. Where bio-available phosphorus is increased by river input, nitrogen concentrations increase as well, except for regions with high denitrification rates. High phosphorus burial rates decrease biological production significantly. Globally, riverine phosphorus leads to elevated primary production rates in the coastal and open oceans.

Plain Language Summary

Coastal oceans are the most productive parts of the global ocean and, arguably, most sensitive to environmental change, but poorly resolved in most global models. In reality, rivers influence the coastal oceans, because they transport nutrients from land to the sea. This nutrient supply is often not included in global models, even though it may impact not only the coastal biology, but also the marine biology in regions farther away. We here include dissolved inorganic nitrogen and phosphorus from river export in a global ocean model and study the effects on the near coastal and the open ocean. We find that the addition of riverine phosphorus affects marine biology on millennial timescales more than riverine nitrogen alone. Where phosphorus is increased by river input, nitrogen concentrations increase as well, except for regions with high rates of bacterial consumption of nitrate (denitrification). High phosphorus burial rates on the other hand, decrease biological production significantly. Globally, riverine phosphorus leads to higher primary production rates in the coastal and open oceans.



25 1 Introduction

Nitrogen and phosphorus are both considered as limiting nutrients in the global ocean, nitrogen as 'proximate limiting' and phosphorus as the 'ultimate limiting', according to the definition by Tyrrell (1999). Changes in the availability of oceanic fixed-nitrogen (N) are known to have driven marine productivity changes, thereby regulating the strength of the biological carbon pump and thereby the partitioning of carbon dioxide (CO₂) between atmosphere and ocean (Falkowski, 1997). Phosphorus (P) is limiting marine productivity on geological and global scales and plays an important role in regulating oceanic oxygen inventories (Monteiro et al., 2012; Palastanga et al., 2011).

Oceanic fixed nitrogen concentrations are mainly controlled by the balance between nitrogen fixation and denitrification, but atmospheric deposition and riverine input also contribute to the global N budget (Somes et al., 2013; Deutsch et al., 2007; Gruber, 2004; Ruttenger, 2003). Although several studies question the stability of the marine N inventory (Zehr and Capone, 2020; Codispoti et al., 2001; Gruber and Sarmiento, 1997; Codispoti, 1995), the pre-industrial global nitrogen cycle is often assumed to reflect a steady state (Deutsch et al., 2007; Altabet, 2006; Gruber, 2004; Tyrrell, 1999; Redfield et al., 1963).

This balance is assured by negative N-cycle feedbacks that stabilize marine N concentration: Where fixed N is sparse, diazotrophs can fix atmospheric N₂ instead of depending on dissolved inorganic nitrogen (DIN), such as ammonia or nitrate. But as the process of atmospheric N fixation is slower and requires more energy, mostly to keep oxygen away from the oxygen-sensitive enzyme nitrogenase, diazotrophs are rapidly outcompeted by other phytoplankton who do not have this energetic cost, if sufficient DIN is available. Growth of diazotrophs is also limited by the availability of phosphate, light and iron.

On the other hand, the global N budget is regulated by loss of fixed N, predominantly via denitrification. This process describes anaerobic respiration of organic matter via bacterial reduction of nitrate to N₂, and occurs in the water column as well as in sediments if the oxygen concentration is low (Gruber, 2004; Deutsch et al., 2001). Denitrification limits itself, as the consumption of nitrate leads to a reduction in the production of organic matter and hence to less oxygen consumption.

Generally the processes of N₂-fixation and denitrification take place in different regions of the world ocean. Still, feedbacks link these processes globally and are generally assumed to restore the balance in the global marine N budget. In some regions, however, N₂-fixation and denitrification occur in geographical proximity and may produce a "vicious cycle" with a runaway local loss of fixed N (Landolfi et al., 2013). Estimates of the mean residence time of fixed nitrogen in the global ocean amount to a few thousand years (Gruber, 2004). Due to the complexity of internal feedbacks and the dynamic role of nitrogen in the marine biological production it is difficult to assess, how sensitive the global N concentration is to perturbations of marine biogeochemistry.

Of particular interest is the interaction between fixed N and phosphorus (P), as P has an impact on the contributors of N cycle feedbacks. P has been termed the 'ultimate' limiting nutrient (compared to the 'proximate' limiting N, citeTyrrell99), and the availability of P is one of the limiting factors for N₂ fixation (Wang et al., 2019; Landolfi et al., 2015).

The total P inventory in the global ocean is mainly controlled by riverine input and burial at the seafloor (Wallmann, 2010;

Ruttenberg, 2003; Baturin, 2003; Delaney, 1998). The residence time of P in the global ocean is approximately one order of magnitude longer than that of fixed N (Delaney, 1998). (Bio-)chemical weathering on continents represents the main source of riverine bio-available P (Filipelli, 2008; Föllmi, 1995). Changes in marine P are mostly a consequence of changes in terrestrial weathering and therefore have generally occurred on geological timescales.

Nevertheless, climate change and direct anthropogenic interventions in the P cycle have started to alter P fluxes during the last century. Due to the wide-spread use of fertilizers, to deforestation and sewage sources, the riverine load of phosphorus has increased globally (Seitzinger et al., 2010; Filipelli, 2008). In addition, river flows have also been dramatically altered by land use change and the damming of rivers (Cappellen and Maavara, 2016). In order to predict future changes in marine biogeochemistry, it is therefore relevant to understand, how P fluxes impact the marine N cycle, the N cycle feedbacks and primary production.

As global observations and measurements of ocean nutrients and fluxes are difficult and observations still relatively sparse, models are often used to investigate large-scale marine biogeochemistry over long time scales. However, only recently have there been more global modelling studies with riverine nutrient input. In one of the first studies, Giraud et al. (2008) analysed coastal fluxes of P, silicate, and dissolved iron in a global ocean model and found that including nutrients in the coastal ocean impacts biological activity locally but also in the open ocean. They also found, that excess nutrients in the coastal ocean can impact the open ocean biogeochemistry depending on which nutrient is advected from the coastal region. Nutrient availability and its consumption in the coastal domain control this advection. Additional P does affect coastal oceans especially if they are P-limited and if they are not limited by other nutrients like iron. In this case, Giraud et al. (2008) found that increased primary production in the coastal oceans can lead to a depletion of nutrients in the open ocean, reducing biological activity there. This "seesaw effect" was detected by Giraud et al. (2008) on local and global scale. If P is not consumed in the coastal oceans, it may be advected offshore, eventually increasing primary production there. N was not simulated explicitly in that study but coupled to P via Redfield ration. In addition, the simulation performed by (Giraud et al., 2008) was only run for 10 years, hence not long enough for N-cycle feedbacks to materialise.

In a more recent study (Lacroix et al., 2020) implemented estimated riverine nutrient loads of P, N, iron, carbon (C) and silica in a global ocean model and compared the results with those by a reference simulation, where the same nutrients were added directly and homogeneously to the open ocean surface. They found that even if the ocean circulation remains the main driver for biogeochemical distributions in the open ocean, it appeared necessary to include riverine inputs for the representation of heterogeneous features in the coastal ocean. They identified the catchments of the tropical Atlantic, the Arctic Ocean, South-east Asia and Indo-Pacific islands as regions of dominant contributions of riverine supplies to the ocean, leading to a strong primary production increase in the tropical west Atlantic, Bay of Bengal and the East China Sea. Nevertheless the focus here was mainly on C export and N feedbacks have not been considered by Lacroix et al. (2020).

In a previous study, we used the Earth system climate model of intermediate complexity of the University of Victoria (UVic) version 2.9 (Eby et al., 2009; Weaver et al., 2001) to study N cycle feedbacks in the modelled ocean in response to the addition of riverine dissolved inorganic nitrogen (Tivig et al., 2021). We found that although marine primary production increased due to the additional N in hot-spots near the river mouths, globally biogeochemical feedbacks stabilized DIN concentrations and



primary production, but could even lead to a local decline in DIN and productivity in proximity to low oxygen regions. In those idealized simulations, N was the only nutrient supplied via rivers.

As P concentrations have been increasing in many water bodies over the world, rivers transport more P to the coastal oceans. Beusen and Bouwman (2022) showed that human-dominated river supply of N and P has not only increased in the past, but will do so in the future, due to legacies of past nutrient management, even if efforts are made to reduce these nutrient loads. Regarding P, not only is the addition of nutrient *per se* relevant for ocean marine biogeochemistry, but the stoichiometric ratio of N and P is also essential for marine biogeochemistry (Garnier et al., 2010; Redfield et al., 1963; Beusen and Bouwman, 2022). In the present study we include riverine supply of both N and P in order to study the feedbacks of the N cycle to the combined input of both limiting nutrients.

Specifically, we address the following questions:

- How does riverine N and P input, rather than riverine N input alone, affect the representation of ocean biogeochemistry including marine primary production in the model?
- How does the addition of riverine P input affect specifically the N cycle and N-cycle feedbacks?
- What effect has the inclusion of riverine P fluxes specifically on marine oxygen concentrations?

To address these questions, an Earth system model of intermediate complexity (EMIC, Claussen et al. (2002)) that resolves the relevant biogeochemical feedbacks is employed. It allows the integration of a large number of processes at reduced computational costs due to a coarser resolution and simplified assumptions, in case of UVic with respect to atmospheric dynamics. This form of model makes it possible to run millennial-scale simulations with different assumptions, allowing the analysis of processes and feedbacks operating in the climate system on such timescales (Weaver et al., 2001).

2 Methods

2.1 Earth system model UVic

The University of Victoria Earth System Climate model (UVic ESCM) version 2.9 (Eby et al., 2009; Weaver et al., 2001) consists of a three-dimensional ($1.8^\circ \times 3.6^\circ$, 19 levels) general circulation model of the ocean, a two-dimensional, single-layer energy-moisture balance atmospheric model, a dynamic-thermodynamic sea ice model, and a terrestrial vegetation model.

The atmospheric energy–moisture balance model (Fanning and Weaver, 1996) dynamically calculates heat and water fluxes between the atmosphere and the ocean, land and sea ice, and is forced by monthly climatological winds prescribed from NCEP/NCAR. The 19 vertical levels of the oceanic component, Modular Ocean Model 2 (MOM2), are 50 m thick near the surface and up to 500 m in the deep ocean. The oceanic physical settings are the same as in Keller et al. (2012). The ocean model includes a marine ecosystem module based on Keller et al. (2012) with updates as noted in Partanen et al. (2016). The ocean ecosystem and biogeochemical model is an improved NPZD (nutrient, phytoplankton, zooplankton, detritus) ecosystem

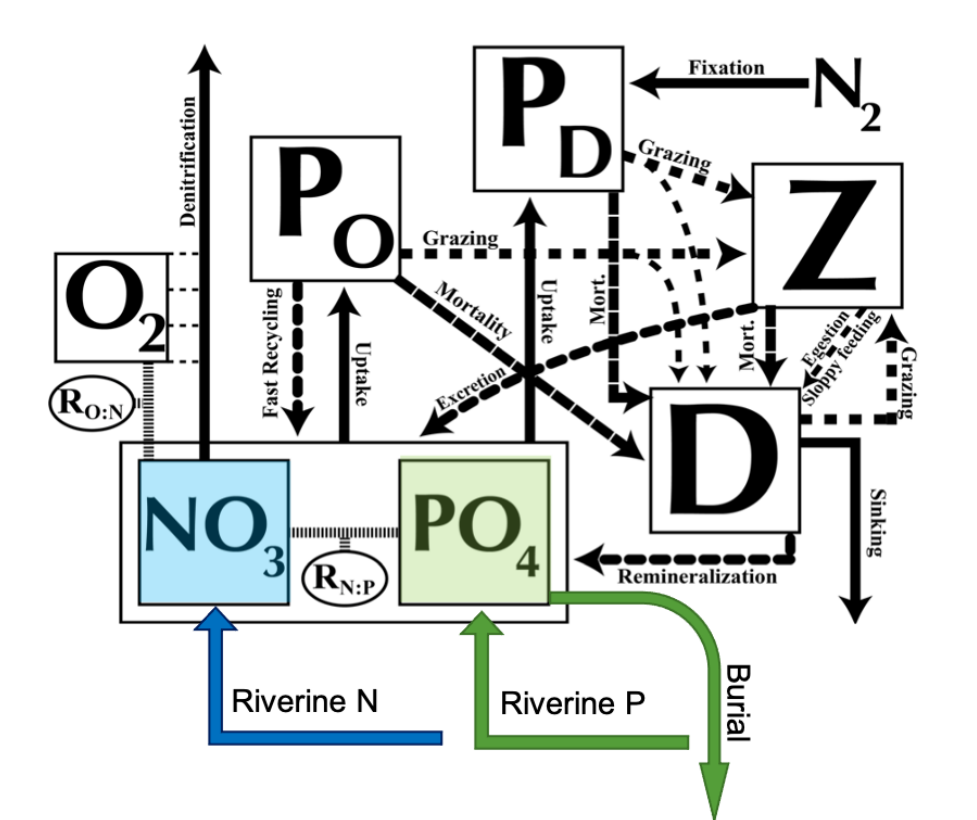


Figure 1. Ecosystem model schematics for the NPZD model with the prognostic variables (in square boxes) and the fluxes of matter between them, indicated by arrows. See details in the text. Figure updated from Keller et al. (2012) and Tivig et al. (2021).

model based on Schmittner et al. (2008) and includes seven prognostic variables: two phytoplankton classes (nitrogen fixing diazotrophs P_D and other phytoplankton P_O), zooplankton (Z), sinking particulate detritus (D), nitrate (NO_3), phosphate (PO_4) and oxygen (O_2) (Fig. 1). NO_3 and PO_4 are linked through exchanges with the biological variables by constant (Redfield) stoichiometry (Schmittner et al., 2008). Since diazotrophs can fix nitrogen gas dissolved in seawater, they are not limited by NO_3 nor by a maximum NO_3 concentration, while the growth of other phytoplankton is limited by NO_3 and PO_4 . All phytoplankton are additionally limited by iron, light and temperature. For the current study of nitrogen cycle feedbacks it is a clear advantage, that UVic explicitly calculates diazotrophs and N_2 -fixation. Keller et al. (2012) found that patterns and global amounts of modelled N_2 fixation were mostly consistent with the relatively sparse available observations (Sohm et al., 2011). The main differences are discussed within the framework of our results. See Keller et al. (2012) for a full description and evaluation of simulated marine biogeochemistry.

As in our previous study (Tivig et al., 2021) we use empirical transfer functions derived from benthic flux measurements to calculate benthic denitrification following Bohlen et al. (2012), combined with a subgrid bathymetry scheme for shallow



135 continental shelves and other topographical features that are too fine to be resolved on the coarse UVic grid (see details in
Somes et al. (2010b)).

2.2 Including riverine Nitrogen and Phosphorus

2.2.1 Global Nutrient Export from WaterSheds 2 (NEWS2)

The basic UVic model and ecosystem module do not account for riverine nutrient input. The only source of N in the ocean
140 model consists in N_2 -fixation. In Tivig et al. (2021) we included riverine N as calculated by a global, spatially explicit model
of nutrient exports by rivers, NEWS2 (Mayorga et al., 2010). This second version of a system of sub-models estimates the
present-day annual export yield at the river mouth for each of 6081 river catchment areas and for dissolved and particulate
forms of organic and inorganic N and P, as well as dissolved organic and particulate carbon. In our model study, parameteriza-
tion of riverine N fluxes is identical to Tivig et al. (2021). Since nitrate is the only nitrogen nutrient explicitly resolved in the
145 UVic version used, all bioavailable N has been included in the nitrate compartment of the model. See Mayorga et al. (2010)
for more details on the model configuration and Dumont et al. (2005) for further details on the validation of NEWS dissolved
inorganic nitrogen (DIN).

2.2.2 Riverine reactive Phosphorus

150 Earlier applications of the UVic ESCM assumed a fixed marine P inventory. In addition to DIN, we here include also P from
river discharge. We here focus on the total amount of reactive P, i.e. that P that exchanges with the dissolved oceanic P-reservoir
and thus is available for biological uptake (Filipelli, 2008; Ruttenger, 2003). Estimates of globally integrated pre-industrial
riverine supply of bioavailable P range from 0.1 Tmol P yr⁻¹ to 0.3 Tmol P yr⁻¹ (Kemena et al., 2019; Ruttenger, 2003;
Filipelli, 2008; Compton et al., 2000; Colman and Holland, 2000). Taking into account only dissolved inorganic P from rivers
155 would underestimate the amount of bioavailable P from river discharge, as most studies estimate DIP export from rivers to be
significantly lower, between 0.01 and 0.05 Tmol P yr⁻¹ (Mayorga et al., 2010; Filipelli, 2008; Harrison et al., 2005). Following
other studies, we decided to include dissolved organic and inorganic P (DOP, DIP), as well as 45 % of total particulate P (TPP).
This represents the upper range of the fraction of riverine TPP flux estimated as reactive-P (Ruttenger, 2003; Colman and
Holland, 2000). The numbers for DIP, DOP and PP export at the river mouths have been taken from the NEWS2 data set.
160 DIP and DOP were taken as such, PP was multiplied by 0.45 to obtain the desired fraction of total particulate P. Consistent
with Tivig et al. (2021), for the current study the nutrients from NEWS2 were interpolated onto the coarser UVic grid. We
assumed a periodic seasonal cycle in runoff and that concentrations in the discharged river water are constant throughout the
seasonal cycle. The annual P load is thus distributed over the months using the fractions of monthly freshwater discharge as
respective weights. The global amount of P we added to the UVic ocean is 0.17 Tmol P yr⁻¹ (5.4 Tg P yr⁻¹), which lays in
165 the range estimated by previous studies (Kemena et al., 2019; Ruttenger, 2003; Benitez-Nelson, 2000). Since phosphate is the



only phosphorus nutrient explicitly resolved in the UVic version used, we decided like for N to put all bioavailable P into the phosphate compartment of the model.

2.2.3 Phosphorus burial

UVic does not contain a prognostic and vertically resolved sediment model. Therefore, the input of reactive P to the ocean has to be counterbalanced by a parameterised sink. For this purpose we included burial functions based on Flögel et al. (2011) and Wallmann (2010), which have been tested in previous studies with UVic by Kemena et al. (2019) and Niemeyer et al. (2017). With these functions, the burial of P in the sediment (BUR_p) is calculated in every ocean grid box column from the difference between the simulated detritus P rain rate to the sediment (RR_p) and the benthic release flux of phosphate from the sediment (BEN_p):

$$175 \quad BUR_p = RR_p - BEN_p, \quad (1)$$

Following Flögel et al. (2011), the burial of P is evaluated separately for each grid box column on the shelf and in the deep-sea. Deep-sea is defined as ocean grid box columns where the ocean is deeper than 1000 m.

Benthic P release (BEN_p) is calculated locally with:

$$BEN_p = \frac{BEN_c}{r_{c/p}}, \quad (2)$$

180 BEN_c represents the benthic fluxes of carbon and was computed from the difference of the carbon rain-rate to the sediment (RR_c) and a virtual burial flux of organic carbon (BUR_c):

$$BEN_c = RR_c - BUR_c, \quad (3)$$

Depending on the ocean depth of the considered grid box, BUR_c is computed from the modelled detritus export in terms of carbon (Kemena et al., 2019). RR_c is in $\text{mmol C m}^{-2} \text{ yr}^{-1}$. The $r_{c/p}$ ratio depends on bottom water oxygen concentration and is calculated following Kemena et al. (2019) and Wallmann (2010):

$$185 \quad r_{c/p} = Y_F - A * \exp(-O_2/r) \quad (4)$$

with O_2 in mmol m^{-3} and the coefficients $Y_F = 123 \pm 24$, $A = -112 \pm 24$ and $r = 32 \pm 19 \text{ mmol m}^{-3}$. Variations in the coefficients determine the strength of the burial. Because there are large uncertainties in these numbers, different experiments have been performed to evaluate the model response to variations in burial.

190 2.3 Experimental design

To analyse the effect of riverine nutrient supply in the UVic model, six experiments were performed (Table 1). In each experiment the model was run for 10,000 years, starting from an already-spun-up steady state with the standard model version without riverine nutrients, with pre-industrial conditions for insolation and a fixed atmospheric CO_2 concentration of 283 ppm



Table 1. Overview of simulations and riverine nutrient fluxes:

Simulation	N-flux in Tg N yr ⁻¹	P-flux in Tg P yr ⁻¹	Description
CTR	0	0	UVic simulation without NEWS (Control)
NEWS-N	22.8	0	UVic simulation with DIN from NEWS
NEWS-P	0	5.4	UVic simulation with P from NEWS, no burial
NEWS-N+P	22.8	5.4	UVic simulation with N and P from NEWS, no burial
N+P-BURLOW	22.8	5.4	UVic simulation with N and P from NEWS, low burial configuration: $Y_F = 100.5$; $A = 90$; $r = 38$. (Kemena et al., 2019)
N+P-BURHIGH	22.8	5.4	UVic simulation with N and P from NEWS, high burial configuration: $Y_F = 123$; $A = 112$; $r = 32$ (Flögel et al., 2011)

(Keller et al., 2012), i.e. a stable climate. All simulations included benthic denitrification and subgrid bathymetry.

195 Like in our previous study Tivig et al. (2021), a control simulation (CTR) was performed without riverine nutrients. The simulation NEWS-N is identical to the main experiment analysed in Tivig et al. (2021), where only DIN from river discharge was added to the coastal ocean. In a follow-up experiment, rivers exported only P to the modelled ocean (NEWS-P), but without any burial to balance the P budget. NEWS-N+P tested the impacts on marine biology and biochemistry with regard to additional N and P (without P burial). Finally, two P burial variation experiments have been performed, where riverine N and P supply from
200 the NEWS2 model was applied. In a low burial configuration (N+P-BURLOW) we used the coefficients tested by Kemena et al. (2019) in their simulation low-bur. The second burial experiment (N+P-BURHIGH) includes the original burial functions of Flögel et al. (2011) with the coefficients for Y_F , A and r described there as well as in the reference burial experiment in Kemena et al. (2019) (Table 1).

Note that previous studies using these burial functions have balanced the modelled P budget by an equivalent weathering flux
205 providing P to the ocean via river discharge in the same amount as P is buried in the marine sediments. In the current study there is no direct link between the two fluxes: riverine P is calculated from the NEWS2 model (Mayorga et al., 2010), while P burial is calculated independently, using only detritus export and bottom-water oxygen concentration (see Table 1 for the overview of the fluxes). In all simulations where riverine P is included, the global P budget is therefore not exactly balanced. The different simulations permit us to analyze the sensitivity of the N cycle feedbacks under different conditions of P supply
210 and do not pretend to reproduce the exact reality. Furthermore, the phosphorus balance of the (pre-anthropogenic) ocean is still poorly defined and the input and output fluxes are only rudimentarily constrained (Wallmann, 2010; Föllmi, 1995).



3 Results

3.1 Phosphorus dynamics

In the four simulations with riverine P input, globally 5.4 Tg P yr⁻¹ (0.17 Tmol P yr⁻¹) are added to the coastal oceans as reactive P, which is close to the amount estimated by Föllmi (1995), and within the range of other literature values for global fluvial fluxes of bioavailable P (Kemena et al., 2019; Ruttenberg, 2003; Benitez-Nelson, 2000; Compton et al., 2000). In NEWS-P and NEWS-N+P no sink of P was implemented, and these simulations are characterized by continually increasing P inventory. Benthic burial fluxes of P amount to 0.16 Tmol yr⁻¹ in N+P-BURLOW and 0.24 Tmol yr⁻¹ in N+P-BURHIGH, leading to an imbalance of +0.01 Tmol yr⁻¹ and -0.07 Tmol yr⁻¹ respectively.

These results range within the estimates for burial rates from observations, which globally vary around 0.2 Tmol P yr⁻¹: 0.11–0.34 Tmol P yr⁻¹ in Benitez-Nelson (2000), 0.17–0.24 Tmol P yr⁻¹ for Ruttenberg (2003) and 0.21 Tmol P yr⁻¹ in Filipelli (2008).

The highest simulated P burial fluxes can be found in coastal regions, especially in the western Pacific and Atlantic ocean (Figure 2). Simulated burial hot spots are situated in proximity to the coast of China, East Russia and Alaska, next to the eastern coast of North- and South-America and in the North Sea. There are no global observational data sets of P burial. Nevertheless, the distribution of the benthic fluxes is similar to other model studies that have used a similar algorithm (e.g. Bohlen et al., 2012).

The inclusion of riverine P has a significant impact on global P concentrations. In simulation CTR without riverine nutrient supply, surface phosphate concentrations range from 0 mmol P m⁻³ in most of the western tropical and subtropical ocean basins to more than 2 mmol P m⁻³ in the Southern Ocean (Figure 3). The addition of riverine N (in NEWS-N) leads only to small changes in the surface P concentrations, in particular P declines reflecting enhanced biological processes (P uptake) in the coastal oceans (Figure 3b). The regions with a decrease in P can be found in the shelf and coastal oceans, corresponding to the regions, where N concentrations are increased in Tivig et al. (2021). Nevertheless, the magnitude of P changes is small compared to the spatial variance of surface phosphate concentrations of 0.64 mmol P m⁻³ in CTR and 0.85 mmol P m⁻³ after 10,000 years of riverine N supply in NEWS-N. For simulations with inclusion of riverine P without benthic burial of P, surface P concentrations after 10,000 years of riverine P supply are much higher than in the control simulation (Figure 3 c. and d.), independent of the additional riverine N supply. Additional P is distributed over the global oceans except for the tropical Atlantic and the north-western tropical Pacific Ocean. These regions correspond to the northern subtropical gyres and are known to be oligotrophic and phosphate limited (Mather et al., 2008; Martiny et al., 2019). The other extreme is the simulation N+P-BURHIGH, where the modelled ocean is losing P in all those regions, where surface P concentrations are different from 0 in CTR (Figure 3 f.). Only moderate changes and a spatial variance of 0.69 mmol P m⁻³ are the result of the simulation with riverine N and P and low burial functions (N+P-BURLOW, Figure 3 e.).

After 10,000 years of simulations with the different scenarios, surface phosphate of N+P-BURLOW appears most similar to observed present-day oceanic conditions. Nevertheless, each scenario provides a different insight in marine biogeochemical feedbacks.

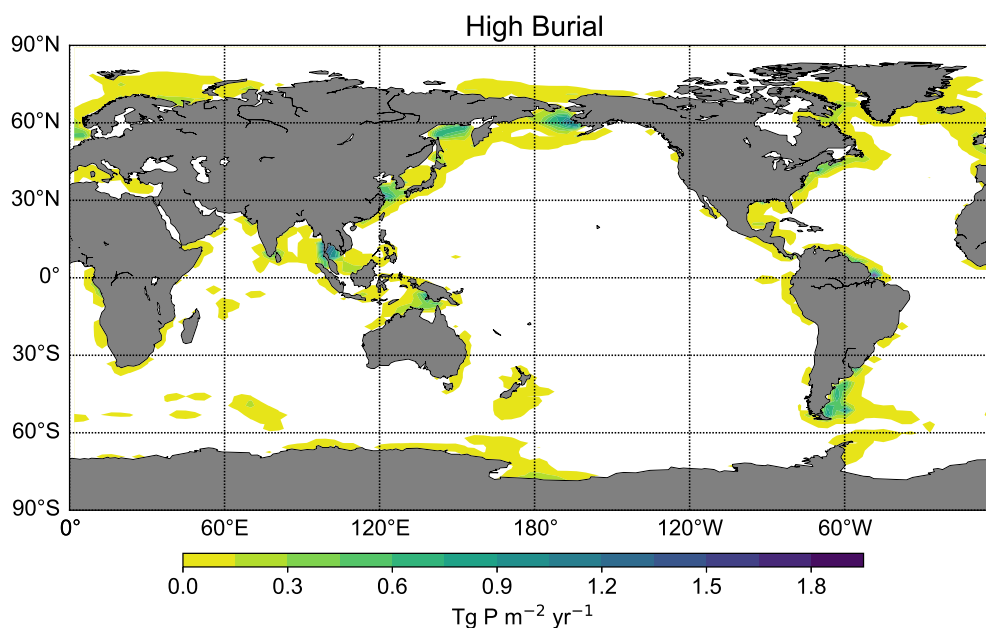


Figure 2. Burial flux of P in the N+P-BURHIGH simulation in g P yr^{-1} .

3.2 P influence on oceanic N inventory and N-cycle feedbacks

The addition of riverine P to the modelled ocean has a considerable impact on the distribution of simulated NO_3 . At the end of CTR, NEWS-N and the simulation N+P-BURLOW, the N sink by denitrification and the N sources by N_2 -fixation and riverine input are balanced (Figure 4). This is not the case for NEWS-P and NEWS-N+P, where the oceanic N inventory slightly increases even at the end of the simulations, and very different from N+P-BURHIGH, where N concentrations decrease continuously. In NEWS-P, where only P is added via river runoff, global oceanic N is only slightly lower than in NEWS-N+P and considerably higher (around 200 Pg N) than in NEWS-N. This is mainly the result of the increase in N-fixation triggered by the additional P flux (Figure 5). Comparing NEWS-N, NEWS-P and N+P-BURLOW shows, that while global benthic denitrification stays nearly constant during the simulations, water column denitrification and N_2 -fixation develop differently depending on the experimental design (Figure 5): additional P leads to an increase in global denitrification and N_2 -fixation. Including burial functions stabilizes both fluxes over time, but at higher levels than in NEWS-N.

Surface NO_3 concentrations increase almost everywhere with supplemental P. Without P burial, N increases globally and especially in the tropical Pacific, the North Atlantic and the higher latitudes, but decreases near the main oxygen minimum zones (OMZ) e.g. in the tropical eastern Pacific because of enhanced denitrification in a more productive ocean. Including P burial leads to smaller N increase, and even a high N decrease as in the simulation with high P burial (Figure 6).

At 300 m depth, NO_3 shows generally higher concentrations compared to the surface, except for the experiments with P burial

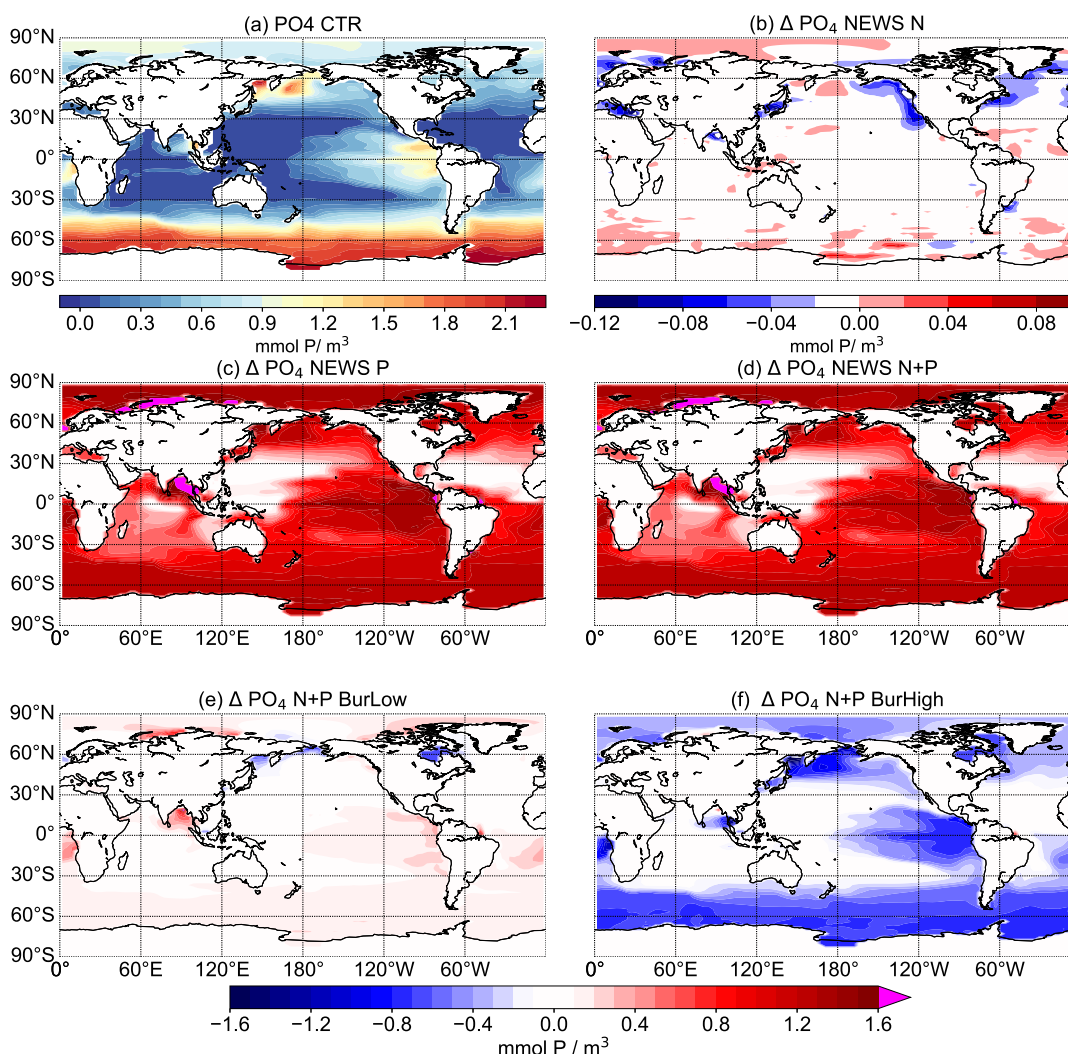


Figure 3. Global distribution of surface PO_4 concentrations in mmol P m^{-3} at the end of the respective simulations over 10,000 years. (a) Global distribution of PO_4 concentrations in CTR. (b)-(f) Difference in PO_4 concentrations between the simulations NEWS-N, NEWS-P, NEWS-N+P, N+P-BURLOW, N+P-BURHIGH compared to CTR. Note the different scale in (b). The magenta colour indicates regions, where the difference in PO_4 concentrations between the respective simulation and CTR is higher than $1.6 \text{ mmol P m}^{-3}$.

and in the OMZs of the Gulf of Guinea, the northern Indian Ocean and the tropical eastern Pacific (Figure 7). Including riverine P has more impact than including riverine N supply alone. If more P is buried, N concentrations decrease globally. The above pattern of N show increasing concentrations almost everywhere in experiment NEWS-P and NEWS-N+P compared to CTR, but is almost reversed for experiment N+P-BURHIGH, with N concentrations at 300 m depth increasing only near the OMZ in

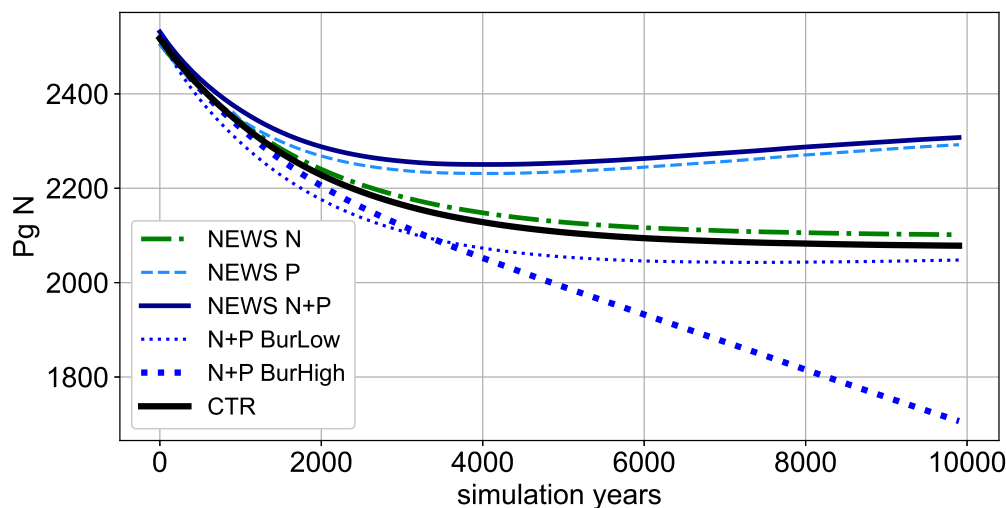


Figure 4. Timeseries of global nitrogen in all simulations over the 10 000 simulation years in Pg N. Simulation description can be found in Table 1.

the Bay of Bengal and off the Pacific coast of Central-America (Figure 7).

270 These changes in NO_3 concentrations are the result of P fluxes impacting the two main processes of the N feedback-cycle, denitrification (Figure 10) and N_2 -fixation (Figure 9). It is widely assumed, that the surface NO_3 to PO_4 ratio is a dominant controlling factor of these feedback mechanisms (Gruber, 2008). Diazotrophs are limited by P, especially in regions, where light, temperature and iron availability are not limiting. The regions where N_2 -fixation is enhanced in the simulations with riverine P (NEWS-P, NEWS-N+P and N+P-BURLOW) corresponds well with regions of general P limitation (compare with (Kemena et al., 2019), Figure 8). N_2 -fixation is stimulated here by the addition of P to the ocean and is generally sensitive to changes in P supply: In the experiment with high burial rates, these same regions are characterized by decreasing N_2 -fixation rates (Figure 9, (f)).

275 Denitrification is the other feedback mechanism controlling the global ocean N budget. In the simulations where N concentration increases due to higher N_2 -fixation rates, denitrification is enhanced as well. In the simulation with high P burial rates on the other hand, denitrification rates are much lower than in the control simulations in the Gulf of Guinea, the Gulf of Bengal and the eastern tropical Pacific (Figure 10, (f)), leading also to higher N concentrations in these regions at 300 m depth (Figure 280 7).

Both processes, N_2 -fixation and denitrification, are increased in the simulation with additional riverine P. Except for the Gulf of Bengal, they take place in different regions of the tropical and subtropical oceans and lead to an increase in DIN in the global surface ocean (N_2 -fixation) and a loss in N in the water columns near the main OMZ of the ocean (denitrification).

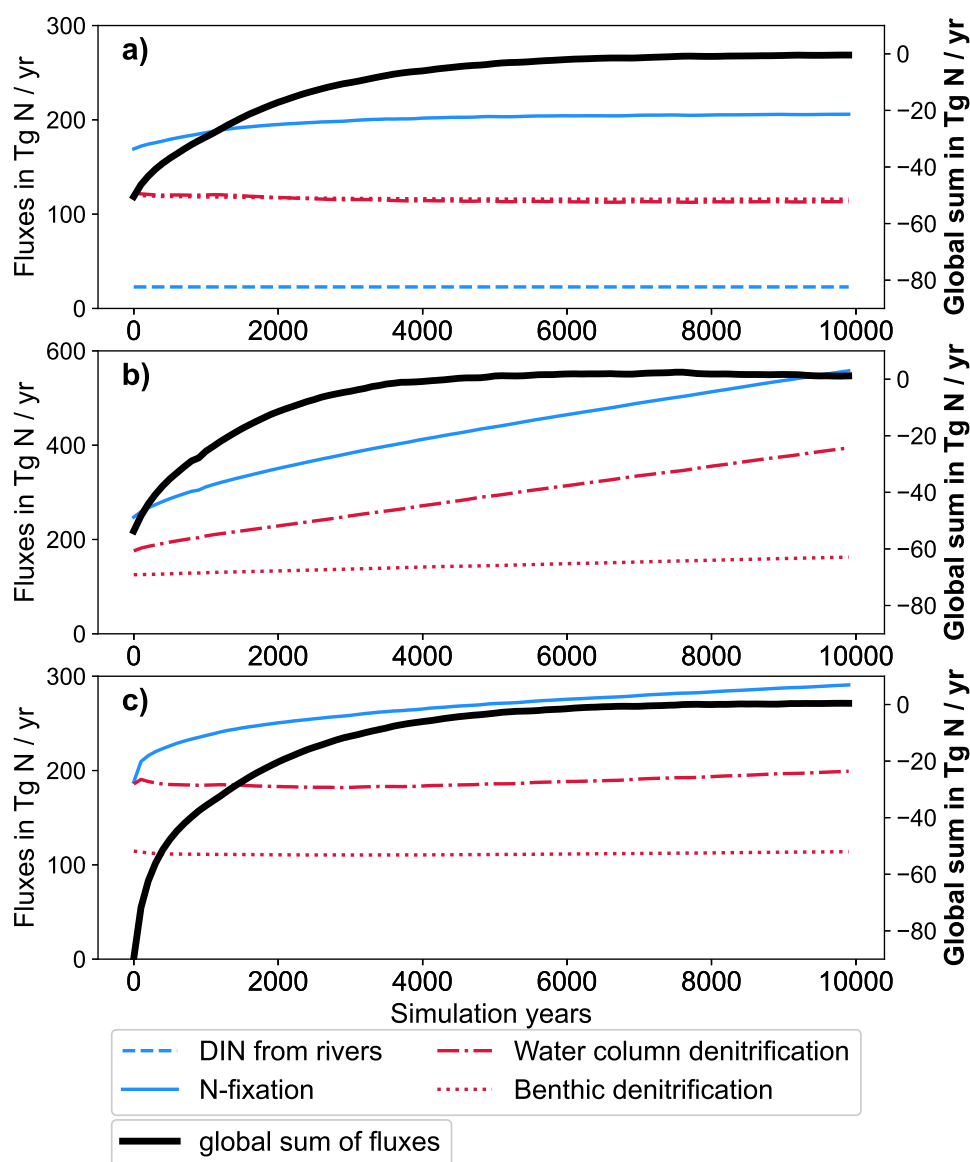


Figure 5. Timeseries of global nitrogen fluxes from NEWS-N (a), NEWS-P (b) and N+P-BURLLOW (c) over the 10 000 simulation years in Tg N per year. Nitrogen fixation (blue solid line) and riverine N input (blue dotted line) are balanced by water column denitrification and benthic denitrification (red solid and red dotted line, respectively). The global sum of all N fluxes is shown as bold black line. Fluxes are given in absolute values. Note the different scales of y-axis.

In our previous study with riverine N only, the "vicious cycle" defined by Landolfi et al. (2013) was suspected to be the reason for a significant decrease in N concentration in the Gulf of Bengal, even though rivers exported additional N to the sea (Figure

285

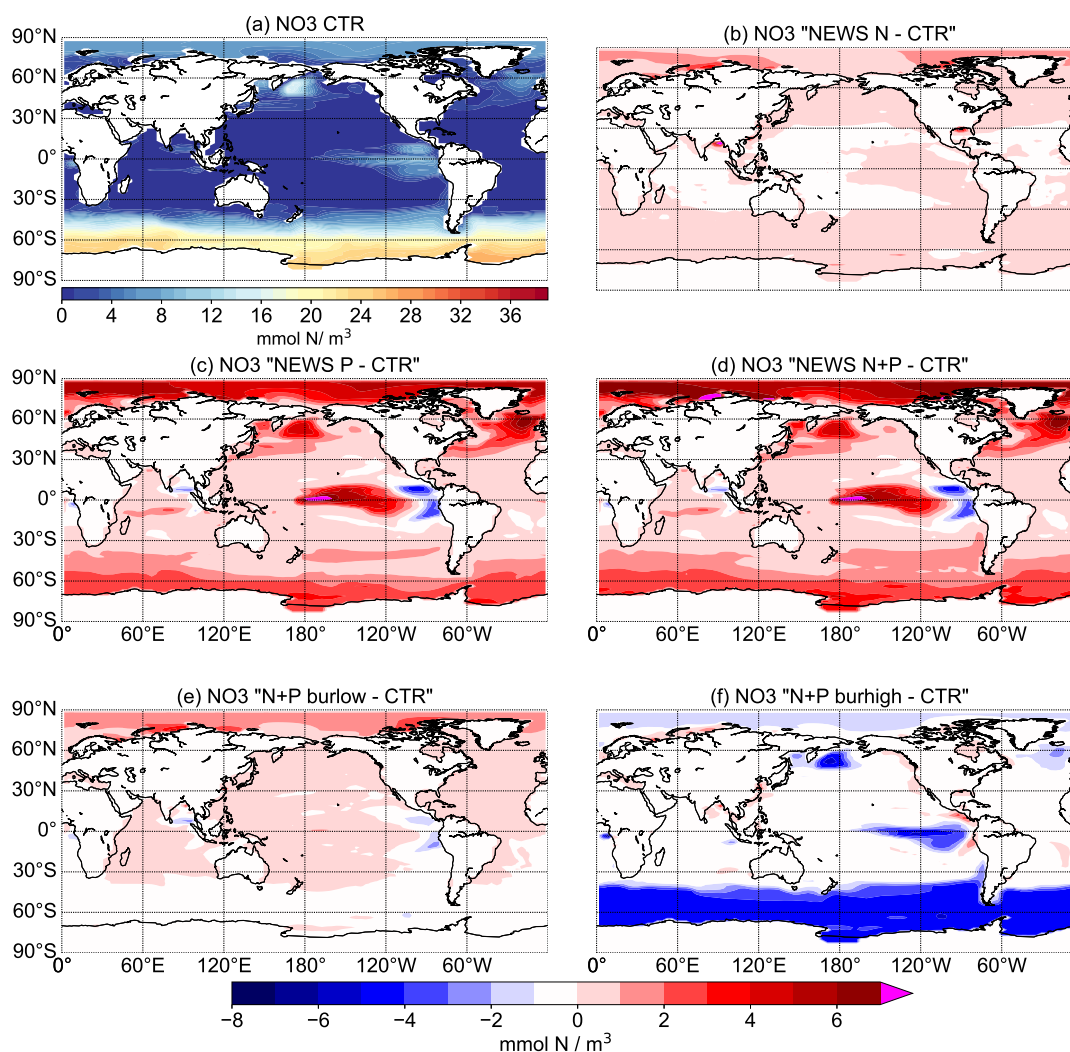


Figure 6. Global distribution of NO_3 concentration at the surface in mmol N m^{-3} . The panel (a) shows NO_3 concentration in CTR. Panels (b)-(f) show N concentration in the simulations NEWS-N, NEWS-P, NEWS-N+P, N+P-BURLOW and N+P-BURHIGH as difference to CTR.

7 (d), Tivig et al. (2021)). Adding riverine P enhances this process here, so that the ocean is losing N not only in the Bay of Bengal, but also in the upper tropical Atlantic ocean basin (Figure 8d,g,j,m) near the Gulf of Guinea and in the upper tropical Pacific ocean (Figure 8e,h,k,n).

The main driver for this vigorous vicious cycle is the P supply from the rivers and the interplay of different feedback loops in these regions of the ocean. Note that iron availability also plays an important role. The model represents iron including a

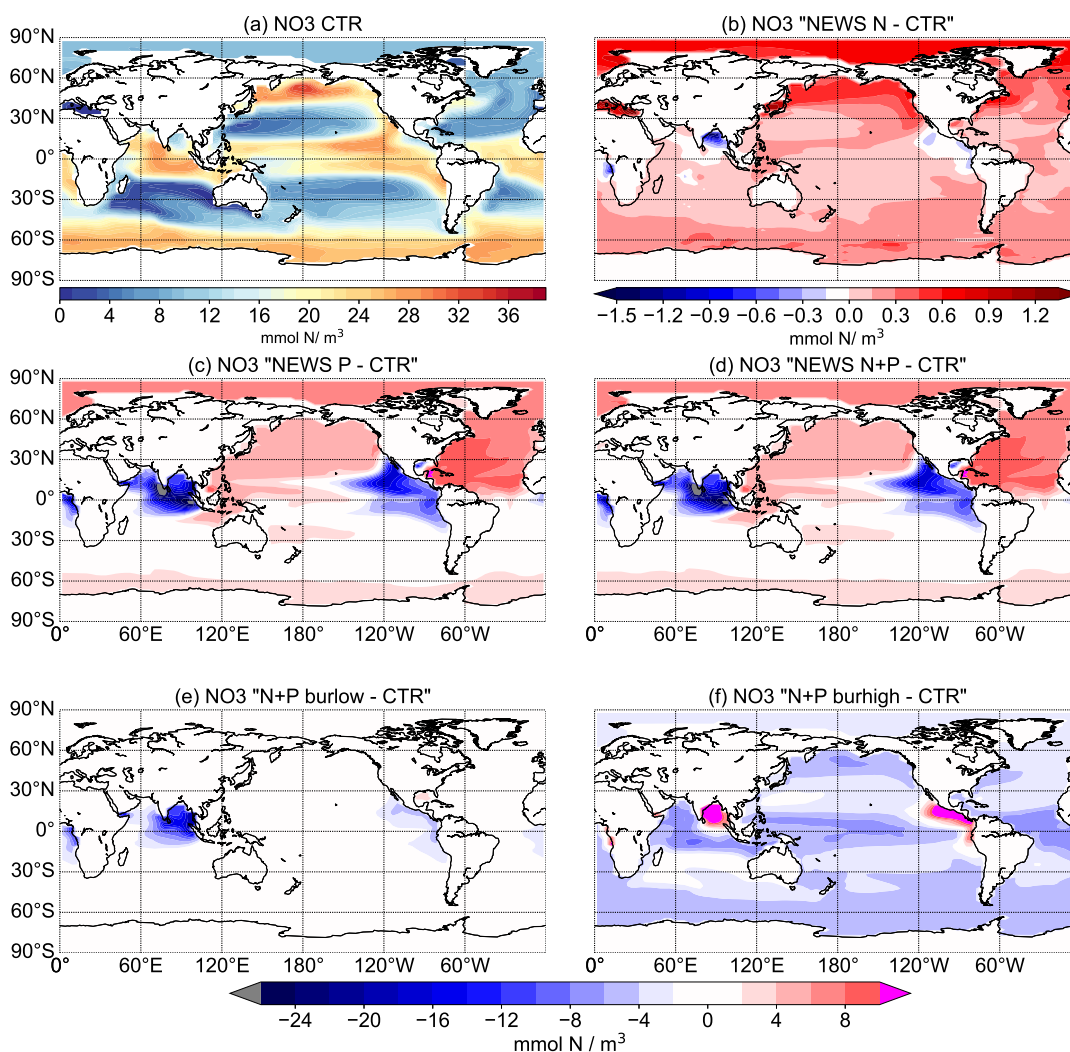


Figure 7. Global distribution of NO_3 concentration at 300 m depth in mmol N m^{-3} . The panel (a) shows NO_3 concentration in CTR. Panels (b)-(f) show N concentration in the simulations NEWS-N, NEWS-P, NEWS-N+P, N+P-BURLOW and N+P-BURHIGH as difference to CTR.

static concentration mask. Therefore no interactive response to perturbations of ocean biogeochemistry are possible and iron availability and limitation will not change during the simulations (Nickelsen et al., 2014). N_2 -fixation is influenced by P only.

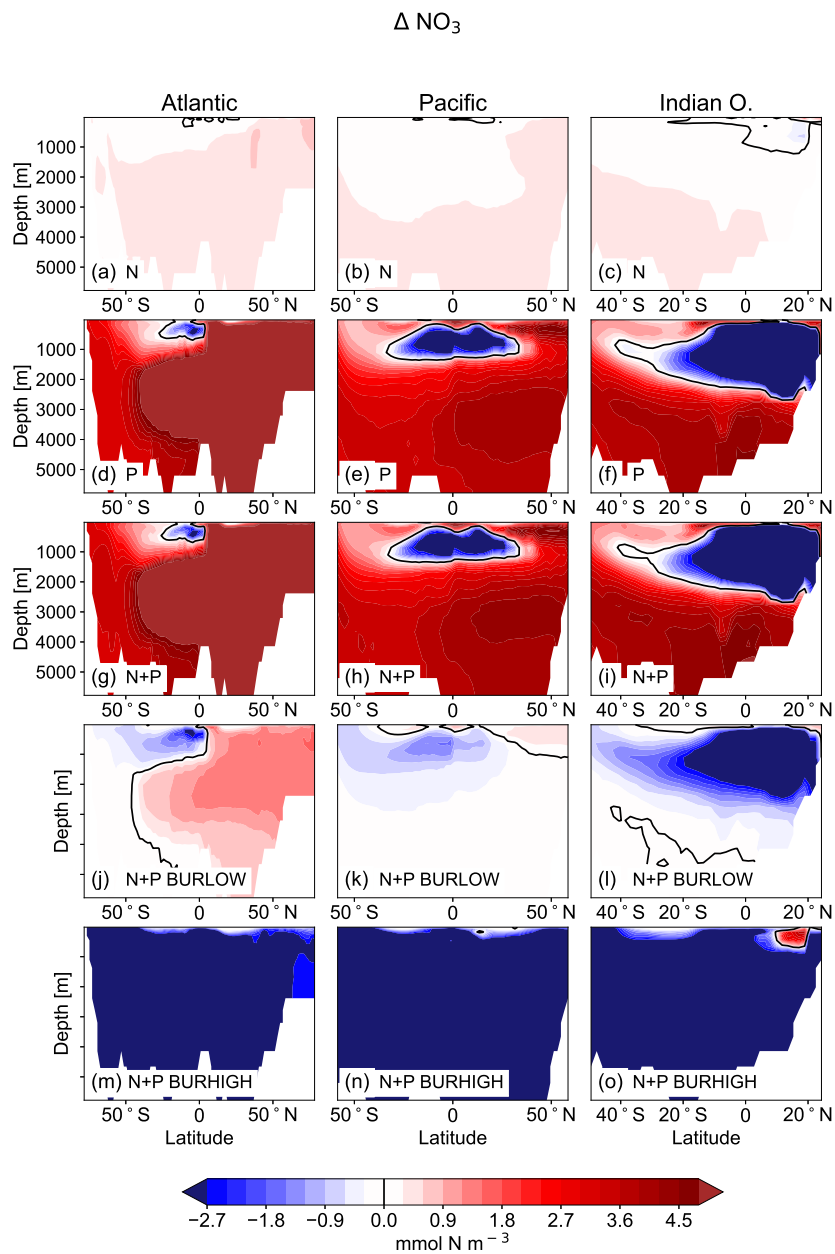


Figure 8. Difference in the zonal mean concentrations of NO_3 in the main ocean basins (Atlantic: left column, Pacific: middle, and Indian Ocean: right) in mmol N m^{-3} as difference between the simulations NEWS-N, NEWS-P, NEWS-N+P, N+P-BURLOW and N+P-BURHIGH and CTR.

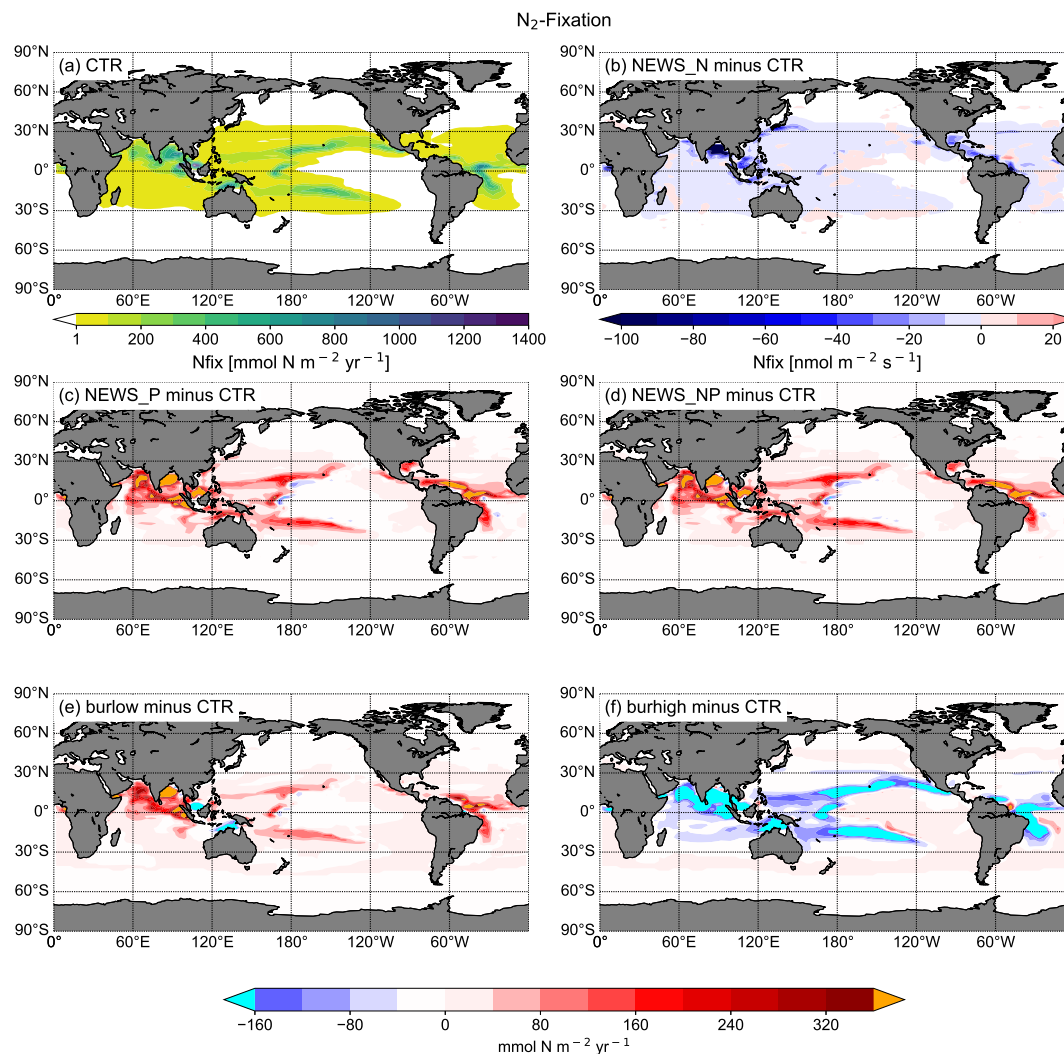


Figure 9. Vertical integration of N₂ fixation in mmol N m⁻² yr⁻¹. (a) N₂ fixation in CTR. (b)-(f) difference in N₂ fixation between the simulations NEWS-N, NEWS-P, NEWS-N+P, N+P-BURLOW and N+P-BURHIGH and CTR. The cyan colour indicates regions with very low N₂ fixation rates compared to CTR. The orange colour indicates regions with very high N₂ fixation rates compared to CTR.

3.3 Phosphorus cycling and oxygen minimum zones

Low ventilation of the water column or high rates of remineralization of organic matter can cause oxygen depleted waters. Niemeyer et al. (2017) found that the increase in the marine phosphorus inventory under assumed business-as-usual global warming conditions could lead to a 4- to 5-fold expansion of the suboxic water volume over millennial timescales. Several



Denitrification

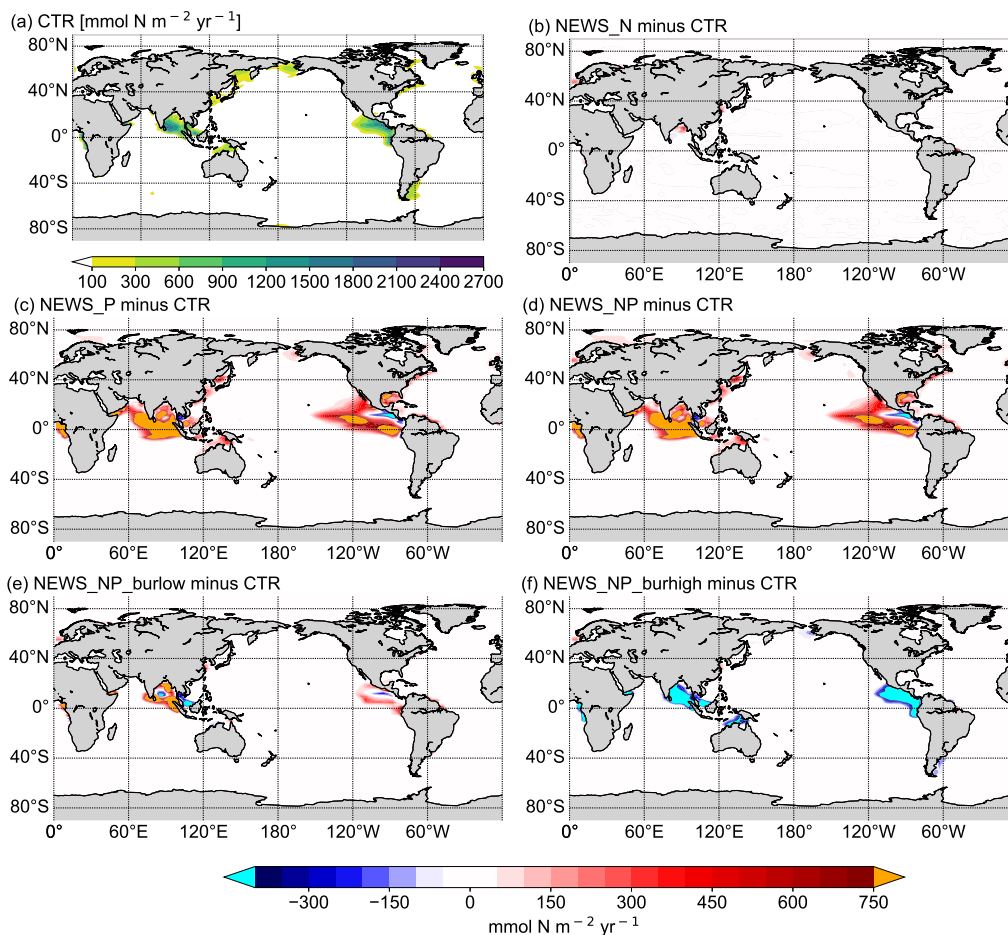


Figure 10. Vertical integration of denitrification in $\text{mmol N m}^{-2} \text{ yr}^{-1}$. (a) Denitrifications rates in CTR. (b)-(f) difference in denitrification rates between the simulations NEWS-N, NEWS-P, NEWS-N+P, N+P-BURLOW and N+P-BURHIGH and CTR. The cyan colour indicates regions with very low denitrification rates compared to CTR. The orange colour indicates regions with very high denitrification rates compared to CTR.

studies also suggest, that O_2 depletion in coastal regions caused by eutrophication may enhance P release from sediments, thereby providing additional P (Flögel et al., 2011; Wallmann, 2010; Ingall and Jahnke, 1994). These two processes together form a positive feedback loop, enhancing oxygen depletion and expansion of the oxygen minimum zones (Oschlies et al., 2018). The processes relevant for this feedback are all included in the experiments with burial.

The three regions, the Gulf of Guinea, the Bay of Bengal and the eastern tropical Pacific ocean are all characterised by low to very low oxygen concentrations (Figure 11a).

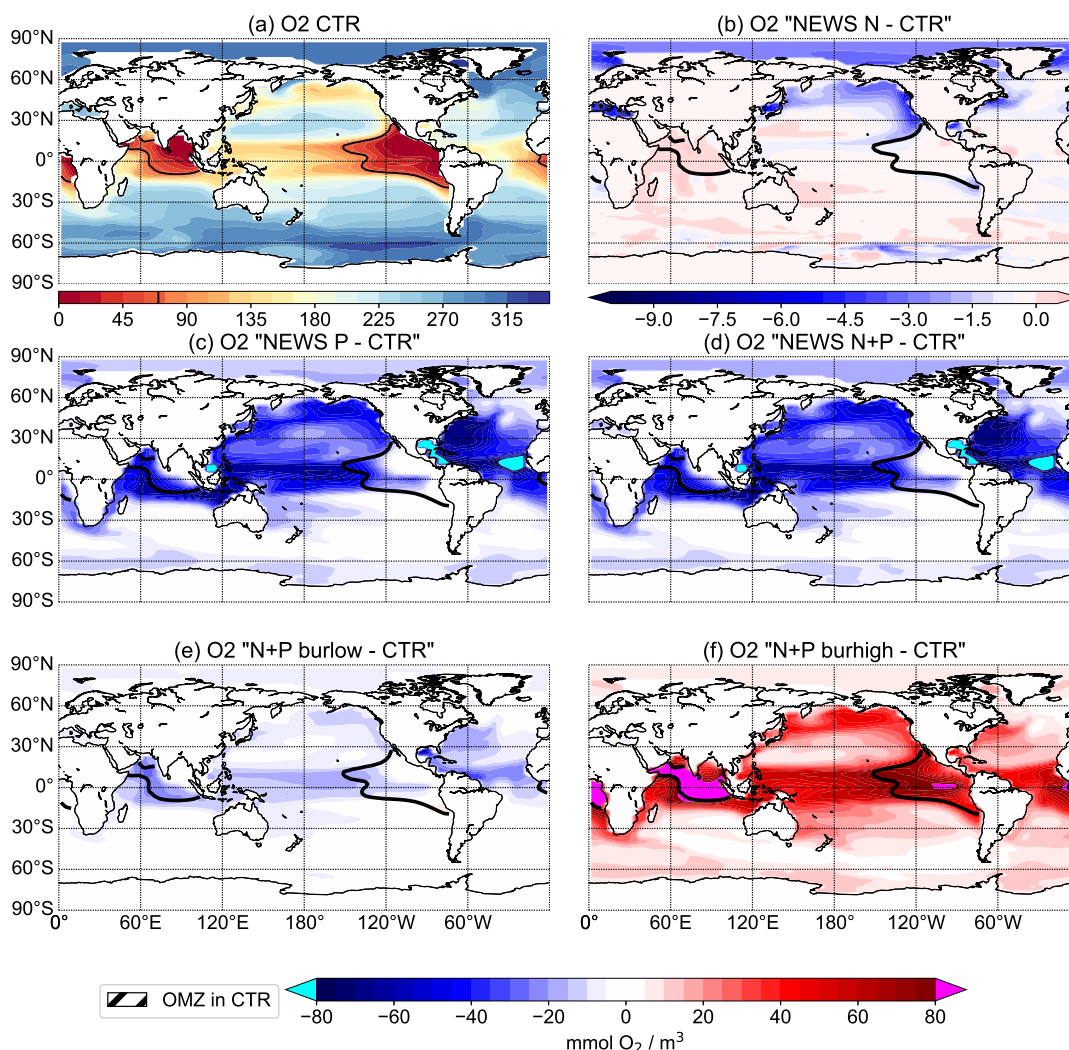


Figure 11. Oxygen concentration at 302 m depth in $\text{mmol O}_2 \text{ m}^{-3}$. (a) distribution of oxygen concentration in the control simulation, difference in oxygen concentration between the simulations NEWS (b), NEWS-P (c), NEWS-N+P (d), PP N+P-BurLOW (e), PP N+P-BurHIGH (f), respectively, and CTR. The black bold line shows the limits of the oxygen minimum zone at 302 m depth in the control simulation.

The black contour lines in Figure 11 indicates the extent of the oxygen minimum zones at 302 m depth, averaged over the last 100 years of the simulations. The oxygen minimum zone is defined here by O_2 concentrations lower than 70 mmol m^{-3} .
 305 The main regions with low oxygen concentrations are known to be situated in subsurface waters of the Arabian Sea and in the areas of the eastern boundary upwelling regions in the tropical oceans off California, Peru and Namibia (Oschlies et al., 2018, e.g.). The model results (Figure 11(a)) show, that UVic misplaces the oxygen minimum zone in the Indian Ocean from the



Arabian Sea to the the Bay of Bengal. This is similar to other biogeochemical ocean models (Séférián et al., 2020). In reality, the Bay of Bengal is a region with strong seasonality driven by the Asian monsoon system (Löscher et al., 2020). Therefore
310 highly variable oxygen concentrations inhibit denitrification while high water column denitrification has been observed in the Arabian Sea (Johnson et al., 2019; Bange et al., 2005).

In the simulations with increased P from rivers oxygen concentrations decrease significantly in all tropical oceans as well as in the eastern boundary regions. P burial damps the oxygen depletion and can even lead to an increase in oxygen concentrations especially in the tropical oceans and in the OMZs (Figure 11). Changes in oxygen concentrations are not limited to oxygen
315 minimum zones and regions do not exactly correlate with regions of changed denitrification rates (Figure 10).

An observational estimate of today's suboxic water area and volume equals 30.4 ± 3 millions of km^2 and 102 ± 15 millions of km^3 respectively, for oxygen concentrations less than 20 mmol m^{-3} (Paulmier and Ruiz-Pino, 2009). In CTR, OMZ defined as regions with oxygen concentration less than 20 mmol m^{-3} (less than 70 mmol m^{-3}) extend to 13.1 millions of km^3 (52 millions of km^3). The addition of riverine N only leads to small changes in oxygen concentrations with a volume of OMZ of
320 13.2 (54) millions of km^3 . Adding P leads to a strong increase in OMZ area with up to a 68 (192) millions of km^3 expansion in NEWS-N+P. With decreased P concentrations, the O_2 concentration increases globally and the global volume of suboxic waters is reduced to less than 1 (5) millions of km^3 . Water column denitrification is mainly controlled by the oxygen concentration (Gruber, 2008). While adding riverine N does not impact the ocean denitrification significantly, the addition of P leads to an increase in denitrification in the three main regions with oxygen deficit waters (Figure 10). Consequently this leads also to
325 reduced N concentrations in these same regions. On the other hand, high P burial rates lead globally to significantly higher O_2 concentrations, decreased rates of denitrification and hence higher N concentrations in regions, where the N cycle feedbacks have limited higher N concentrations before (Figure 7 (f)). Including N from rivers only slightly impacts the O_2 distribution, but can lead to a negative feedback loop near oxygen minimum zones. In our first experiment this phenomenon also impacted primary production in these regions, damping a global increase in marine production compared to the control simulation.
330 Adding P from riverine export to the modelled ocean leads to much more changes in N and in the oxygen concentration. As O_2 plays an important role in the N feedback cycles, the impact is more significant and not only reduced to the OMZ (refer also to Figure 12).

3.4 Primary Production

In Tivig et al. (2021) we showed, that including riverine N had only limited impact on marine productivity, due at least
335 partially to feedback reactions in the marine N cycle. Additional P changes this result significantly (Figure 13): Comparing the simulation with riverine N only to the simulation with riverine P only shows that, at least in our model and on a millennial timescale, P is more limiting for primary production than N alone. Primary production amounts to 67 Pg C yr^{-1} globally in NEWS-P compared to only 55 Pg C yr^{-1} in NEWS-N. Even in the low burial simulation, marine biology is more productive than in the simulation without riverine P addition (59 Tg C yr^{-1}). In N+P-BURHIGH on the other hand, where the ocean is
340 deprived from P at the end of the simulation, production rates decrease in the global tropical oceans to reach a global integral 33 Pg C yr^{-1} . Only near the river mouths, where burial has not been effective yet, NPP rates are higher than in the control

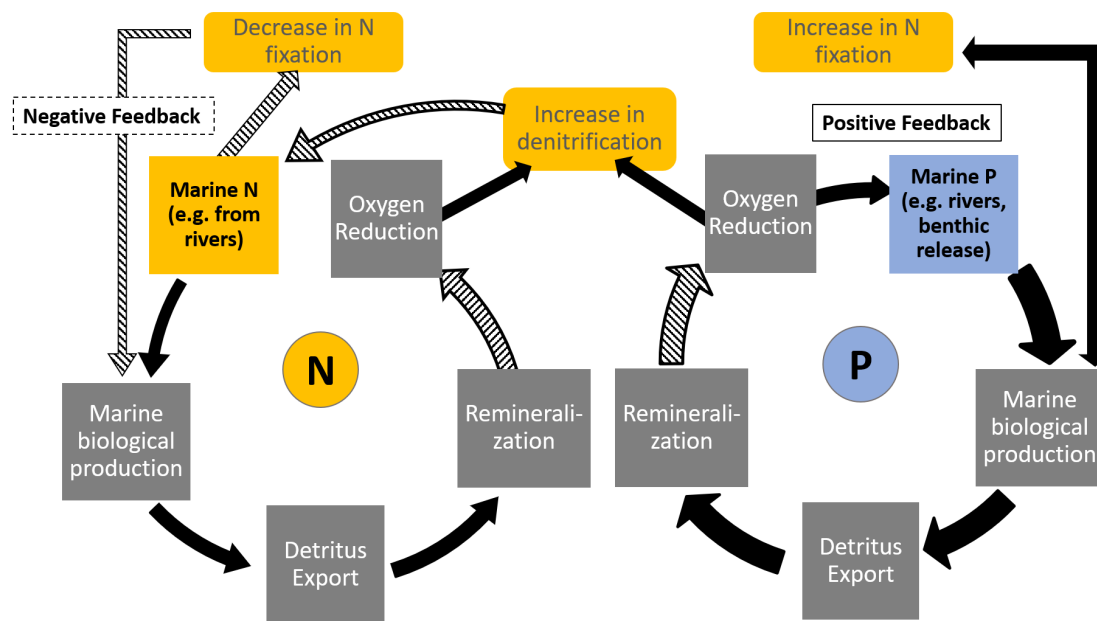


Figure 12. Feedbacks in the marine N and P cycle. Yellow colored boxes refer to processes concerning the marine N inventory. Blue refers to the marine P inventory. The black arrows symbolise positive relations or feedbacks. The dashed arrows symbolise negative relations or feedbacks.

simulation. To summarize, NPP rates are sensitive to P addition in our model. In the simulations with N and P addition from rivers, the feedbacks are still active, but NPP rates are nevertheless higher than in our simulation with riverine N alone.

4 Conclusions

345 In this follow-up study to Tivig et al. (2021), a new component was added to the global Earth system model UVic, that had been employed before to simulate the effects of N supply from river discharge. In the current study, riverine phosphorus has been included separately and in addition to N. After 10,000 years only a simulation with low P burial rates reached a steady state. Nevertheless, all simulations showed that including riverine P in the model has more impact on the modelled marine biogeochemistry and biology than the inclusion of N alone. Therefore, we can answer the questions raised at the start:

- 350 – After 10,000 years of simulations, the global amount of P in the ocean has increased significantly in the simulations where riverine P is not balanced by burial sinks and continues to increase by 5.4 Tg P yr^{-1} . In the simulation with low burial rates, global P increase only by 0.5 Tg P yr^{-1} , while the simulation with high burial rates leads to a loss in global P by $-2.1 \text{ Tg P yr}^{-1}$.

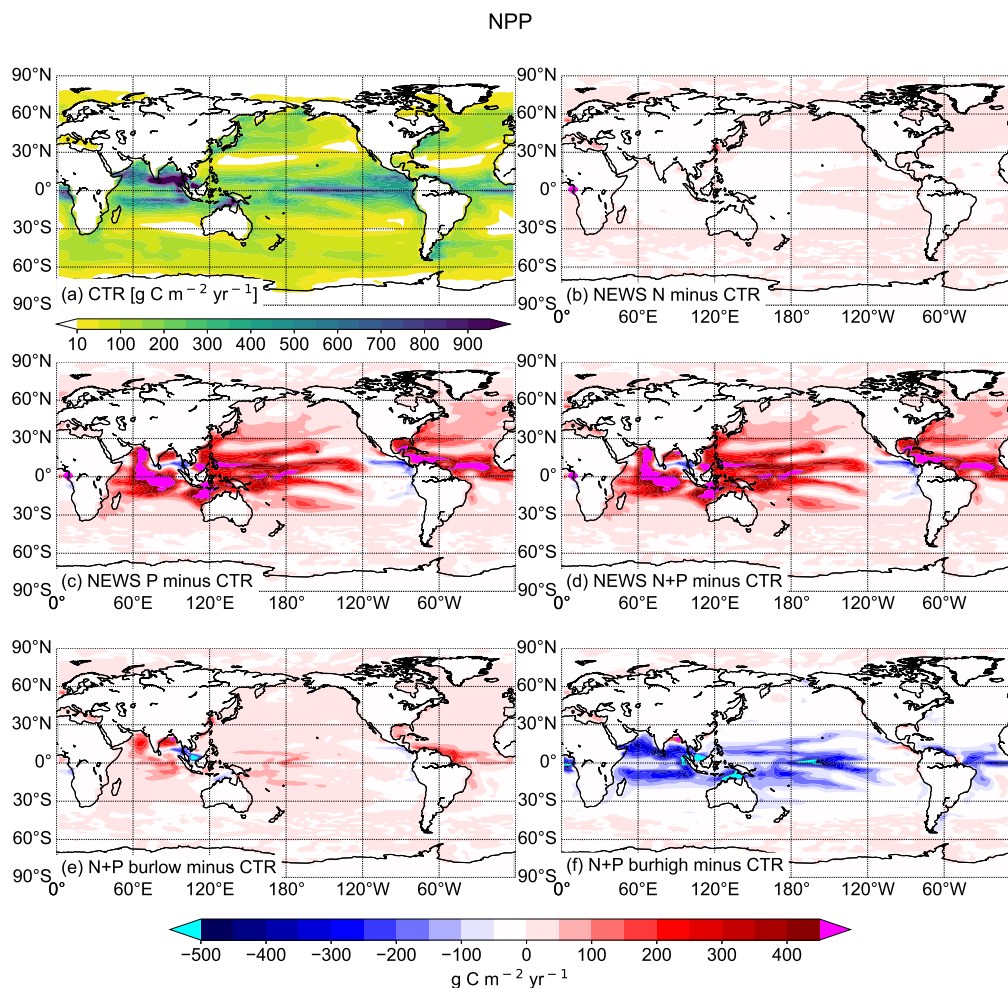


Figure 13. Vertical integration of primary production in $\text{g C m}^{-2} \text{ yr}^{-1}$.

- 355
- The additional P affects marine biology not only near the river mouths but also in regions far off the coasts and in the deep oceans.
 - Because the additional P (as well as the loss of P in N+P-BURHIGH) affects the two processes denitrification and N_2 -fixation, the N-cycle is also affected and N concentration increases or decreases locally and globally. In simulations where P is added without burial, N concentrations also increase globally, except in regions where denitrification is dominant, in proximity to regions with low to very low oxygen concentrations. Balancing the addition of P by P burial leads to a
- 360
- decrease in the global marine N concentration. The global amount of N at the end of the 10,000 years is lower than at



the start of the burial simulations (by -1.5 % in N+P-BURLOW and -18.2 % in N+P-BURHIGH). This can be attributed to the so called "vicious cycle", triggered here by higher N and P supply in proximity to low oxygen regions.

365 – Adding P in the coastal oceans has significant impact on marine oxygen concentrations. Simulated oxygen concentrations decrease globally but more in the tropical and Nordic oceans, if P is added without an additional sink. In the simulation where P is lost due to sediment burial, however, O₂ concentrations increase in the whole oceans. In Tivig et al. (2021) we found, that O₂ concentrations is only slightly impacted by the addition of riverine N alone.

370 Finally our study showed that additional P from riverine input strongly influences marine productivity not only in the coastal oceans, but also in the open oceans worldwide. Our model simulations suggest that, on millennial timescales, the impact of riverine P on ocean biogeochemistry is more important than the one of riverine N. While this result is linked to our model configuration, it is nevertheless relevant for the real ocean. The main sources of P as the “ultimately limiting nutrient” are rivers transporting P provided by weathering and human activities (Giraud et al., 2008; Föllmi, 1995). While weathering processes are active on millennial timescales and therefore only slowly change the amount of P advected by the rivers, human activities have influenced these nutrient transports more rapidly during the last centuries (Beusen et al., 2016). Additionally, changes in atmospheric carbon dioxide concentrations and resulting climate changes have already and will in the future impact riverine 375 export as well as ocean biogeochemistry (Gao et al., 2023). Although the uncertainties in the real and the modelled nutrient fluxes are still large, our simulation suggests that global ocean biogeochemistry can be affected by the supply of nutrients from rivers and that the global representation of biological activity may be improved by considering riverine export and coastal processes. For this purpose, a better spatial resolution of the coastal oceans as well as more realistic representation of coastal N and P cycling processes could be helpful.

380 *Code and data availability.* The data and material that support the findings of this study are available through GEOMAR at <https://hdl.handle.net/20.500.12085/85adfd5-bc86-440c-a205-496749a9025f> (Tivig et al., 2024). More information on the original NEWS2 data set is available from the Global NEWS group at the web site http://icr.ioc-unesco.org/index.php?option=com_content&view=article&id=45&Itemid=100002. Please email Emilio Mayorga at mayorga@marine.rutgers.edu to obtain this data set.

385 *Author contributions.* MT developed the research concept in discussion with AO and DPK. DPK provided the initial model code, which was further developed, run, and analysed by MT. MT analysed the model output and visualised the results. MT wrote the manuscript with contributions from all co-authors.

Competing interests. The authors declare that they have no conflict of interest.



Acknowledgements. We gratefully acknowledge E. Mayorga, S. Seitzinger and their co-authors for making their database of Global Nutrient Export from WaterSheds 2 (NEWS2) available for our study. AO and DPK acknowledge funding from the European Union's Horizon 2020 Research and Innovation Program under grant 820989 (project COMFORT, "Our common future ocean in the Earth system — quantifying coupled cycles of carbon, oxygen, and nutrients for determining and achieving safe operating spaces with respect to tipping points") and OceanNETs (grant no. #869357). The work reflects only the author's view; the European Commission and their executive agency are not responsible for any use that may be made of the information the work contains. This work was also supported by the German Research Foundation (DFG) as part of the research project SFB 754 "Climate-Biogeochemistry Interactions in the Tropical Ocean". We would also

390
395



References

- Altabet, M. A.: Constraints on oceanic N balance/imbalance from sedimentary 15N records, *Biogeosciences*, 4, 75–86, <https://doi.org/10.5194/bg-4-75-2007>, 2006.
- 400 Bange, H., Naqvi, S., and Codispoti, L.: The nitrogen cycle in the Arabian Sea, *Progress in Oceanography*, 65(2-4), 145–158, <https://doi.org/10.1016/j.pocean.2005.03.002>, 2005.
- Baturin, G. N.: Phosphorus Cycle in the Ocean, *Lithology and Mineral Resources*, 38, 101–119, 2003.
- Benitez-Nelson, C. R.: The biogeochemical cycling of phosphorus in marine systems, *Earth-Science Reviews*, 51, 109–135, [https://doi.org/10.1016/S0012-8252\(00\)00018-0](https://doi.org/10.1016/S0012-8252(00)00018-0), 2000.
- 405 Beusen, A. H. W. and Bouwman, A. F.: Future projections of river nutrient export to the global coastal ocean show persisting nitrogen and phosphorus distortion, *Frontiers:Water*, 4, 893 585, <https://doi.org/10.3389/frwa.2022.893585>, 2022.
- Beusen, A. H. W., Bouwman, A. F., Beek, L. P. H. V., Mogollon, J. M., and Middelburg, J. J.: Global riverine N and P transport to ocean increased during the 20th century despite increased retention along the aquatic continuum, *Biogeosciences*, 13, 2441–2451, <https://doi.org/10.5194/bg-13-2441-2016>, 2016.
- 410 Bohlen, L., Dale, A. W., and Wallmann, K.: Simple transfer functions for calculating benthic fixed nitrogen losses and C:N:P regeneration ratios in global biogeochemical models, *Global Biogeochemical Cycles*, 26, GB3029, <https://doi.org/10.1029/2011GB004198>, 2012.
- Cappellen, P. V. and Maavara, T.: Rivers in the Anthropocene: Global scale modifications of riverine nutrient fluxes by damming, *Ecology Hydrobiology*, 16, 106–111, 2016.
- Claussen, M., Mysak, L. A., Weaver, A. J., Crucifix, M., Fichet, T., Loutre, M.-F., Weber, S., Alcamo, J., Alexeev, V., Berger, A.,
415 Calov, R., Ganopolski, A., Goosse, H., Lohmann, G., Lunkeit, F., Mokhov, I., Petoukhov, V., Stone, P., and Wang, Z.: Earth System Models of Intermediate Complexity: Closing the Gap in the Spectrum of Climate System Models, *Climate Dynamics*, 18, 579–586, <https://doi.org/10.1007/s00382-001-0200-1>, 2002.
- Codispoti, L. A.: Is the ocean losing nitrate?, *Nature*, 376, 1995.
- Codispoti, L. A., Brandes, J. A., Christensen, J. P., Devol, A. H., Naqvi, S. A., Paerl, H. W., and Yoshinari, T.: The oceanic fixed nitrogen
420 and nitrous oxide budgets: Moving targets as we enter the anthropocene?, *Scientia Marina*, 65, 85–105, 2001.
- Colman, A. S. and Holland, H. D.: The Global Diagenetic Flux of Phosphorus from Marine Sediments to the Oceans: Redox Sensitivity and the Control of Atmospheric Oxygen Levels., in: *Marine Authigenesis: From Global to Microbial*, vol. 66, p. 53–75, SEPM Society for Sedimentary Geology, <https://doi.org/10.2110/pec.00.66.0053>, 2000.
- Compton, J., Mallinson, D., Glenn, C. R., Filippelli, G., Föllmi, K., Shields, G., and Zanin, Y.: Variations in the global phos-
425 phorus cycle, in: *Marine Authigenesis: From Global to Microbial*, vol. 66, pp. 21–33., SEPM Society for Sedimentary Geology, <https://doi.org/10.2110/pec.00.66.0021>, 2000.
- Delaney, M. L.: Phosphorus accumulation in marine sediments and the oceanic phosphorus cycle, *Global Biogeochemical Cycles*, 12 No.4, 563–572, 1998.
- Deutsch, C., Gruber, N., Key, R. M., and Sarmiento, J. L.: Denitrification and N₂ fixation in the Pacific Ocean, *Global Biogeochemical
430 Cycles*, 15, 483–506, 2001.
- Deutsch, C., Sarmiento, J. L., Sigman, D. M., Gruber, N., and Dunne, J. P.: Spatial coupling of nitrogen inputs and losses in the ocean, *Nature*, 445, 163–167, 2007.



- Dumont, E., Harrison, J. A., Kroeze, C., Bakker, E. J., and Seitzinger, S. P.: Impacts of Atmospheric Anthropogenic Nitrogen on the Open Ocean, *Global Biogeochemical Cycles*, 19, GB4S02, <https://doi.org/10.1029/2005GB002488>, 2005.
- 435 Eby, M., Zickfeld, K., Montenegro, A., Archer, D., Meissner, K. J., and Weaver, A. J.: Lifetime of Anthropogenic Climate Change: Millennial Time Scales of Potential CO₂ and Surface Temperature Perturbations, *Journal of Climate*, 22, 2501–2511, <https://doi.org/10.1175/2008JCLI2554.1>, 2009.
- Falkowski, P. G.: Evolution of the nitrogen cycle and its influence on the biological sequestration of CO₂ in the ocean, *Nature*, 387, 272–275, <https://doi.org/10.1038/387272a0>, 1997.
- 440 Fanning, A. F. and Weaver, A. J.: An atmospheric energy-moisture balance model: Climatology, interpentadal climate change, and coupling to an ocean general circulation model, *Journal of Geophysical Research*, 101, 15 111–15 128, <https://doi.org/10.1029/96JD01017>, 1996.
- Filipelli, G. M.: The Global Phosphorus Cycle: Past, Present, and Future, *Elements*, 4, 89–95, <https://doi.org/10.2113/GSELEMENTS.4.2.89>, 2008.
- Flögel, S., Wallmann, K., Poulson, C. J., Zhou, J., Oschlies, A., Voigt, S., and Kuhnt, W.: Simulating the biogeochemical effects of volcanic CO₂ degassing on the oxygen-state of the deep ocean during the Cenomanian/Turonian Anoxic Event (OAE2), *Earth Planet Scientific Letters*, 305, 371–384, <https://doi.org/10.1016/j.epsl.2011.03.0181>, 2011.
- 445 Föllmi, K. B.: The Phosphorus Cycle, phosphogenesis and marine phosphate-rich deposits, *Earth-Science Reviews*, 40, 55–124, [https://doi.org/10.1016/0012-8252\(95\)00049-6](https://doi.org/10.1016/0012-8252(95)00049-6), 1995.
- Gao, S., Schwinger, J., Tjiputra, J., Bethke, I., Hartmann, J., Mayorga, E., and Heinze, C.: Riverine impact on future projections of marine primary production and carbon uptake, *Biogeochemistry*, 20, 93–119, <https://doi.org/10.5194/bg-20-93-2023>, 2023.
- 450 Garnier, J., Beusen, A., Thieu, V., Billen, G., and Bouwman, L.: N:P:Si nutrient export ratios and ecological consequences in coastal seas evaluated by the ICEP approach, *Global Biogeochemical Cycles*, 24, GB0A05, <https://doi.org/10.1029/2009GB003583>, 2010.
- Giraud, X., Quéré, C. L., and da Cunha, L. C.: Importance of coastal nutrient supply for global ocean biogeochemistry, *Global Biogeochemical Cycles*, 22, GB2025, <https://doi.org/10.1029/2006GB002717>, 2008.
- 455 Gruber, N.: The Dynamics of the Marine Nitrogen Cycle and its Influence on Atmospheric CO₂ Variations, in: *The Ocean Carbon Cycle and Climate*, edited by Follows, M. and Oguz, T., pp. 97–148, Springer Netherlands, Dordrecht, https://doi.org/10.1007/978-1-4020-2087-2_4, 2004.
- Gruber, N.: The marine nitrogen cycle: Overview and challenges, in: *Nitrogen in the Marine Environment*, edited by et al., D. G. C., chap. 1, pp. 1–50, Academic Press, San Diego, California, 2 edn., 2008.
- 460 Gruber, N. and Sarmiento, J. L.: Global patterns of marine nitrogen fixation and denitrification, *Global Biogeochemical Cycles*, 11, 235–266, <https://doi.org/10.1029/97GB00077>, 1997.
- Harrison, J. A., Seitzinger, S. P., Bouwman, A. F., Caraco, N. F., Beusen, A. H. W., and Vörösmarty, C. J.: Dissolved inorganic phosphorus export to the coastal zone: Results from a spatially explicit, global model, *Global Biogeochemical Cycles*, 19, GB4S03, <https://doi.org/10.1029/2004GB002357>, 2005.
- 465 Ingall, E. and Jahnke, R.: Evidence for enhanced phosphorus regeneration from marine sediments overlain by oxygen depleted waters, *Geochimica et Cosmochimica Acta*, 58, 2571–2575, 1994.
- Johnson, K. S., Riser, S. C., and Ravichandran, M.: Oxygen Variability Controls Denitrification in the Bay of Bengal Oxygen Minimum Zone, *Geophysical Research Letters*, 46, 804–811, <https://doi.org/10.1029/2018GL079881>, 2019.
- Keller, D. P., Oschlies, A., and Eby, M.: A new marine ecosystem model for the University of Victoria Earth System Climate Model, *Geoscientific Model Development*, 5, 1195–1220, <https://doi.org/10.5194/gmd-5-1195-2012>, 2012.
- 470



- Kemena, T. P., Landolfi, A., Oschlies, A., Wallmann, K., and Dale, A. W.: Ocean phosphorus inventory: large uncertainties in future projections on millennial timescales and their consequences for ocean deoxygenation, *Earth System Dynamics*, 10, 539–553, <https://doi.org/10.5194/esd-10-539-2019>, 2019.
- Lacroix, F., Ilyina, T., and Hartmann, J.: Oceanic CO₂ outgassing and biological production hotspots induced by pre-industrial river loads of nutrients and carbon in a global modeling approach, *Biogeosciences*, 17, 55–88, <https://doi.org/10.5194/bg-17-55-2020>, 2020.
- Landolfi, A., Dietze, H., Koeve, W., and Oschlies, A.: Overlooked runaway feedback in the marine nitrogen cycle: the vicious cycle, *Biogeosciences*, 10, 1351–1363, <https://doi.org/10.5194/bg-10-1351-2013>, 2013.
- Landolfi, A., Koeve, W., Dietze, H., Kähler, P., and Oschlies, A.: A new perspective on environmental controls of marine nitrogen fixation, *Geophysical Research Letters*, 42, 4482–4489, <https://doi.org/10.1002/2015GL063756>, 2015.
- 480 Löscher, C. R., Mohr, W., Bange, H. W., and Canfield, D. E.: No nitrogen fixation in the Bay of Bengal?, *Biogeosciences*, 17, 851–864, <https://doi.org/10.5194/bg-17-851-2020>, 2020.
- Martiny, A. C., Lomas, M. W., Fu, W., Boyd, P. W., Chen, Y.-I. L., Cutter, G., Ellwood, M. J., Furuya, K., Hashihama, F., Kanda, J., Karl, D. M., Kodama, T., Li, Q. P., Ma, J., Moutin, T., Woodward, E. M. S., and Moore, J. K.: Biogeochemical controls of surface ocean phosphate, *Science Advances*, 5, eaax0341, <https://doi.org/10.1126/sciadv.aax0341>, 2019.
- 485 Mather, R. L., Reynolds, S. E., Wolff, G. A., Williams, R. G., Torres-Valdes, S., Woodward, E. M. S., Landolfi, A., Pan, X., Sanders, R., and Achterberg, E. P.: Phosphorus cycling in the North and South Atlantic Ocean subtropical gyres, *Nature Geoscience*, 1, 439–443, <https://doi.org/10.1038/ngeo232>, 2008.
- Mayorga, E., Seitzinger, S. P., Harrison, J. A., Dumont, E., Beusen, A. H. W., Bouwman, A., Fekete, B. M., Kroeze, C., and van Drecht, G.: Global Nutrient Export from WaterSheds 2 (NEWS 2): Model development and implementation, *Environmental Modelling and Software*, 490 25, 837–853, <https://doi.org/10.1016/j.envsoft.2010.01.007>, 2010.
- Monteiro, F. M., Pancost, R. D., Ridgwell, A., and Donnadieu, Y.: Nutrients as the dominant control on the spread of anoxia and euxinia across the Cenomanian-Turonian oceanic anoxic event (OAE2): Model-data comparison, *Paleoceanography*, 27, PA4209, <https://doi.org/10.1029/2012PA002351>, 2012.
- Nickelsen, L., Keller, D., and Oschlies, A.: A dynamic marine iron cycle module coupled to the University of Victoria Earth System Model: the Kiel Marine Biogeochemical Model 2 (KMBM2) for UVic 2.9, *Geoscientific Model Development Discussions*, 7, 8505–8563, <https://doi.org/10.5194/gmdd-7-8505-2014>, 2014.
- 495 Niemeyer, D., Kemena, T. P., Meissner, K. J., and Oschlies, A.: A model study of warming-induced phosphorus–oxygen feedbacks in open-ocean oxygen minimum zones on millennial timescales, *Earth System Dynamics*, 8, 357–367, <https://doi.org/10.5194/esd-8-357-2017>, 2017.
- 500 Oschlies, A., PBrandt, Stramma, L., and Schmidtko, S.: Drivers and mechanisms of ocean deoxygenation, *Nature Geoscience*, 11, 467–473, <https://doi.org/10.1038/s41561-018-0152-2>, 2018.
- Palastanga, V., Slomp, C. P., and Heinze, C.: Long-term controls on ocean phosphorus and oxygen in a global biogeochemical model, *Global Biogeochemical Cycles*, 25, GB3024, <https://doi.org/10.1029/2010GB003827>, 2011.
- Partanen, A.-I., Keller, D. P., Korhonen, H., and Matthews, H. D.: Impacts of sea spray geoengineering on ocean biogeochemistry, *Geophysical Research Letters*, 43, 7600–7608, <https://doi.org/10.1002/2016GL070111>, 2016.
- 505 Paulmier, A. and Ruiz-Pino, D.: Oxygen minimum zones (OMZs) in the modern ocean, *Global Biogeochemical Cycles*, 25, GB3024, <https://doi.org/10.1016/j.pocan.2008.08.001>, 2009.



- Redfield, A. C., Ketchum, B. H., and Richards, F. A.: The Influence of Organisms on the Composition of Sea-Water, in: *The Sea Vol. 2*, edited by Hill, M. N., pp. 26–27, Interscience, New York, 1963.
- 510 Ruttenger, K. C.: The Global Phosphorus Cycle, in: *Treatise on Geochemistry*, edited by Schlesinger, W., Elsevier, <https://doi.org/https://doi.org/10.1016/B0-08-043751-6/08153-6>, 2003.
- Schmittner, A., Oschlies, A., Matthews, H. D., and Galbraith, E. D.: Future changes in climate, ocean circulation, ecosystems, and biogeochemical cycling simulated for a business-as-usual CO₂ emission scenario until year 4000 AD, *Global Biogeochemical Cycles*, 22, GB1013, <https://doi.org/10.1029/2007GB002953>, 2008.
- 515 Seitzinger, S. P., Mayorga, E., Bouwman, A. F., Kroeze, C., Beusen, A. H. W., Billen, G., Drecht, G. V., Dumont, E., Fekete, B. M., Garnier, J., and Harrison, J. A.: Global river nutrient export: A scenario analysis of past and future trends, *Global Biogeochemical Cycles*, 24, GB0A08, <https://doi.org/10.1029/2009GB003587>, 2010.
- Sohm, J. A., Webb, E. A., and Capone, D. G.: Emerging patterns of marine nitrogen fixation, *Nature Reviews Microbiology*, 9, 499–508, <https://doi.org/10.1038/nrmicro2594>, 2011.
- 520 Somes, C. J., Schmittner, A., Galbraith, E. D., Lehmann, M. F., Altabet, M. A., Montoya, J. P., Letelier, R. M., Mix, A. C., Bourbonnais, A., and Eby, M.: Simulating the global distribution of nitrogen isotopes in the ocean, *Global Biogeochemical Cycles*, 24, GB4019, <https://doi.org/10.1029/2009GB003767>, 2010b.
- Somes, C. J., Oschlies, A., and Schmittner, A.: Isotopic constraints on the pre-industrial oceanic nitrogen budget, *Biogeosciences*, 10, 5889–5910, <https://doi.org/10.5194/bg-10-5889-2013>, 2013.
- 525 S  ferian, R., Berthet, S., Yool, A., Palmi  ri, J., Bopp, L., Tagliabue, A., Kwiatkowski, L., Aumont, O., Christian, J., Dunne, J., Gehlen, M., Ilyina, T., John, J. G., Li, H., Long, M. C., Luo, J. Y., Nakano, H., Romanou, A., Schwinger, J., Stock, C., Santana-Falc  n, Y., Takano, Y., Tjiputra, J., Tsujino, H., Watanabe, M., Wu, T., Wu, F., and Yamamoto, A.: Tracking Improvement in Simulated Marine Biogeochemistry Between CMIP5 and CMIP6, *Current Climate Change Reports*, 6, 95–119, <https://doi.org/10.1007/s40641-020-00160-0>, 2020.
- Tivig, M., Keller, D. P., and Oschlies, A.: Riverine nitrogen supply to the global ocean and its limited impact on global primary production: a feedback study using an Earth system model, *Biogeosciences*, 18, 5327–5350, <https://doi.org/10.5194/bg-18-5327-2021>, 2021.
- 530 Tivig, M., Keller, D. P., and Oschlies, A.: UVic simulation with riverine nutrient export from NEWS2 dataset., <https://doi.org/hdl:20.500.12085/85adfd5-bc86-440c-a205-496749a9025f>, 2024.
- Tyrrell, T.: The relative influences of nitrogen and phosphorus on oceanic primary production, *Nature*, 400, 525–531, 1999.
- Wallmann, K.: Phosphorus imbalance in the global ocean?, *Global Biogeochemical Cycles*, 24, GB4030, <https://doi.org/10.1029/2009GB003643>, 2010.
- 535 Wang, W.-L., Moore, J. K., Martiny, A. C., and Primeau, F. W.: Convergent estimates of marine nitrogen fixation, *Nature*, 566, 205–211, <https://doi.org/10.1038/s41586-019-0911-2>, 2019.
- Weaver, A. J., Eby, M., Wiebe, E. C., Bitz, C., Duffy, P. B., Ewen, T. L., Fanning, A. F., Holland, M. M., MacFadyen, A., Matthews, H. D., Meissner, K. J., Saenko, O., Schmittner, A., Wang, H., and Yoshimori, M.: The UVic Earth System Climate Model: Model Description, Climatology, and Applications to Past, Present and Future Climates, *Atmosphere-ocean*, 39(4), 361–428, <https://doi.org/10.1080/07055900.2001.9649686>, 2001.
- 540 Zehr, J. P. and Capone, G.: Changing perspectives in marine nitrogen fixation, *Science*, 368, <https://doi.org/10.1126/science.aay9514>, 2020.